Journal of Solid State Chemistry **159,** 72–79 (2001)
doi:10.1006/jssc.2001.9133, available online at http://www.idealibrary.com on IDEAL®

The Upper Limit of the Solid Solution $Bi_{2-x}Sb_xMoO_6$: Structure Refinement of $Bi_{1.1}Sb_{0.9}MoO_6$

P. Bégué,* R. Enjalbert,† and A. Castro*,[1]

*Instituto de Ciencia de Materiales de Madrid, CSIC, Cantoblanco, 28049 Madrid, Spain; and †Centre d'Elaboration de Matériaux et d'Etudes Structurales, CNRS, 29 rue Jeanne Marvig, B.P. 4347, 31055 Toulouse Cedex 4, France

Received November 8, 2000; in revised form January 26, 2001; accepted February 15, 2001; published online May 4, 2001

The crystal structure of $Bi_{1.1}Sb_{0.9}MoO_6$ has been refined using X-ray and neutron powder diffraction combined with Rietveld analysis. This oxide is isostructural with the high-temperature form of Bi_2MoO_6 (γ(H)) belonging to the monoclinic system, space group $P2_1/c$, $a = 17.0988(7)$ Å, $b = 22.3342(9)$ Å, $c = 5.5679(2)$ Å, $\beta = 90.926(3)^\circ$, $V = 2126.0(1)$ Å^3, $Z = 16$, and $\rho_{cal} = 6.64$ g.cm^{-3}. The phase stoichiometry has been verified and constitutes the upper limit of the $Bi_{2-x}Sb_xMoO_6$ solid solution. Antimony atoms progressively go to bismuth sites in an ordered way that can be understood according to Bi/Sb–O observed distances and the stereoactivity of $5s^2$ and $6s^2$ lone pair of electrons of Sb^{3+} and Bi^{3+}, respectively. The maximum $x = 0.9$ substitution value for this solid solution is explained on the basis of the bond-valence method. The Bi/Sb–O bond valence generally decreases with increasing antimony content, reaching strongly underbonded Bi/Sb–O states beyond which the substitution cannot progress. © 2001 Academic Press

Key Words: **bismuth; molybdenum; antimony; substitution; oxides; solid solution; X-ray; neutron; powder diffraction; stereochemistry.**

INTRODUCTION

Recently the synthesis of two new solid solutions, $Bi_{2-x}Sb_xMoO_6$ and $Bi_{2-y}As_yMoO_6$, has been reported (1). These oxides were prepared by solid-state reaction as powdered samples, with x and y values ranging from 0 to 0.9 and to 0.4, respectively. In the same way, single crystals of both Sb- and As-substituted oxides have been grown by a flux method, showing that the upper substitution limit for single crystals is 0.4 in both cases, while the upper limit for powdered $Bi_{2-x}Sb_xMoO_6$ phases is 0.9.

Structural studies on these compounds show that they belong to the γ(H) Bi_2MoO_6 structural type. This is the most interesting material of the Bi_2O_3–MoO_3 system. In fact, Bi_2MoO_6 exhibits four polymorphic phases that are obtained at increasing temperatures, depending on the synthesis protocol. For the sake of clarity the Kodama and Watanabe (2) notation is used in the present work to identify every phase. The γ(F) phase, showing a fluorite-like structure, is a low-temperature metastable phase and can only be obtained from a mechanochemically activated precursor mixture of oxides (3). The γ(L) phase is currently obtained by a solid-state reaction method, transforming reversibly to γ(I) at moderate temperature (4–6); both phases show a layered Aurivillius-type structure, although the γ(I) structure is not well characterized. Electrical and structural studies carried out by the present authors seem to reveal that the γ(L)$\leftrightarrow\gamma$(I) Bi_2MoO_6 transition is due to a ferroparaelectric transition; these results will be reported in the near future. Finally, the γ(H) Bi_2MoO_6 phase is obtained by heating at moderate temperature the other Bi_2MoO_6 polymorphs, and it remains stable on cooling. Its structure shows an original arrangement built up by columns and ribbons of Bi–O linked to independent MoO_4 tetrahedra, as was determined by X-ray single-crystal and neutron powder diffraction techniques (1,7).

The Bi–Mo–O phases are mainly known as very good catalysts for alkene ammoxidation or hydrocarbon oxidation reactions (see for example Refs. (7) and (8)). The Bi_2MoO_6 oxide is considered to be one of the most interesting materials in this system in view of its different applications as ionic conductor (10), ferroelectric material (11), and also catalyst (12). Since all these properties are closely related to the structure and composition of this kind of material, the study of the structure of the members of the new solid solution $Bi_{2-x}Sb_xMoO_6$ recently reported (1) seems to be of interest. Unfortunately, the upper limit of such a solid solution, $x = 0.9$, could not be isolated as single crystals (1) and thus its structural characteristics remain unknown. So, this work reports the structural study, by coupling X-ray and neutron powder diffraction techniques, and characterization of the $Bi_{1.1}Sb_{0.9}MoO_6$ oxide. This study affords an opportunity to show evidence of the preferential occupation

[1] To whom correspondence should be addressed. Fax: (34) 91 372 06 23. E-mail: acastro@icmm.csic.es.

0022-4596/01 $35.00

of Bi^{3+} sites by Sb^{3+}, according to their stereochemical behavior.

EXPERIMENTAL

1. Sample Preparation and Characterization

The $Bi_{1.1}Sb_{0.9}MoO_6$ oxide was prepared by solid state reaction from a ground mixture of Bi_2O_3, Sb_2O_3, and MoO_3 of analytical grade, in the stoichiometric proportion Bi : Sb : Mo 1.1 : 0.9 : 1. The mixture was heated at increasing temperatures from 400 to 550°C, for periods of 12 h, in evacuated quartz ampoules to prevent the partial oxidation of Sb^{3+} to Sb^{5+}. The final powder was found to be a well-crystallized single phase.

Thermal stability of $Bi_{1.1}Sb_{0.9}MoO_6$ was studied by thermogravimetry (TG) and differential thermal analysis (DTA). TG and DTA curves were recorded under N_2 to prevent Sb^{3+} oxidation, up to 800°C on a Seiko 320 instrument at a heating/cooling rate of 10°C min^{-1}. About 10 mg of sample was used for each run, with Al_2O_3 used as reference material.

Density measurements were carried out on the powdered sample in an Accupyc 1330 pycnometer using the helium displacement technique.

2. X-Ray and Neutron Powder Diffraction

The purity of the sample was checked by X-ray diffraction using a Siemens Kristalloflex 810 generator and a D-501 goniometer equipped with a graphite monochromator to select the Cu $K\alpha$ radiation ($\lambda = 1.5418$ Å). The data were recorded between 5° and 65° (2θ) at increments of 0.05° (2θ) and counting time of 1 second per step. Additional X-ray data were collected for the refinement of the structure with the same diffractometer, at room temperature, but in this case the data were recorded between 5° and 120° (2θ) with an increment of 0.02° (2θ) and counting time of 10 seconds per step.

Neutron data were recorded at room temperature on the powder diffractometer D1A at the Institut Laue Langevin in Grenoble. A wavelength of 1.910 Å was selected from a Ge monochromator. The pattern was recorded with increments of 0.05° (2θ) and 250 seconds of counting time, between 10° and 150° (2θ).

In both cases the structure was refined by the Rietveld method, using the program Fullprof (13). No regions were excluded in the refinement. Details about the refinement procedure are given in the next section.

RESULTS

Characterization of the Oxide

The sample with the composition $Bi_{1.1}Sb_{0.9}MoO_6$ was dark green and showed a clean X-ray diffraction pattern characteristic of the γ(H) Bi_2MoO_6 structural type. The DTA and TG curves show that this material remains unaltered up to 700°C; beyond this temperature incongruent melting and decomposition of the product occur. That is one of the reasons it is impossibile for single crystals to grow with high antimony content in the solid solution $Bi_{2-x}Sb_xMoO_6$ (1) from the melt.

The measured density of $Bi_{1.1}Sb_{0.9}MoO_6$ was $\rho_{exp} = 6.64(2)$ g cm^{-3}, in agreement with a unit cell volume of $V = 2126$ Å^3, which is typical of the γ(H) Bi_2MoO_6 structure, for $Z = 16$. On the basis of such results a refinement of the structure of this highly substituted material was undertaken by using both X-ray and neutron powder diffraction techniques.

Refinement of the Structure

As it has been mentioned, $Bi_{1.1}Sb_{0.9}MoO_6$ is isostructural with the high-temperature polymorph of Bi_2MoO_6. Its powder diffraction pattern can be completely indexed on the basis of a monoclinic cell with $a \approx 17.10$ Å, $b \approx 22.30$ Å, $c \approx 5.57$ Å, and $\beta \approx 90.9°$, belonging to space group $P2_1/c$. The refinement of the $Bi_{1.1}Sb_{0.9}MoO_6$ structure (Fig. 1) was undertaken starting from the structural model previously reported (1,7).

In the first stage the X-ray diffraction data were used to refine the unit cell parameters, the cation coordinates, and the occupancy parameters for the different Bi/Sb sites, which allowed verification of the antimony:bismuth ratio. No attempt was made to refine the oxygen sites, and they were left fixed. In the final stage of the refinement a total of 58 parameters were varied freely, including the coordinates of Mo and Bi/Sb atoms and the occupation of Bi/Sb1 to Bi/Sb6. The occupations of Bi/Sb7 and Bi8 were fixed to the determined values found in previous refinement cycles, 0.34/0.66 and 1, respectively, in order to stabilize the refinement and improve the overall fit. The background was computed with the usual polynomial function and a pseudo-Voigt profile function was used for peak fitting. The final profile and Bragg agreement factors are reported in Table 1 together with the unit cell parameters for this $Bi_{1.1}Sb_{0.9}MoO_6$ oxide. The final refined coordinate values and occupation factors are given in Table 2. Parameters given without the standard deviations were not refined.

Structural refinement from neutron data was carried out in the same way, except that the positional parameters of oxygen atoms and thermal parameters for all atoms were also refined during the last cycles, with a total of 126 fitted parameters. In contrast, the occupancy site values obtained from X-ray refinement were fixed for neutron refinement. Results of this refinement are reported in Tables 1 and 2 and selected interatomic distances presented in Table 3. The observed and calculated diffraction patterns are shown in Fig. 2a for X-ray and in Fig. 2b for neutron refinements, respectively.

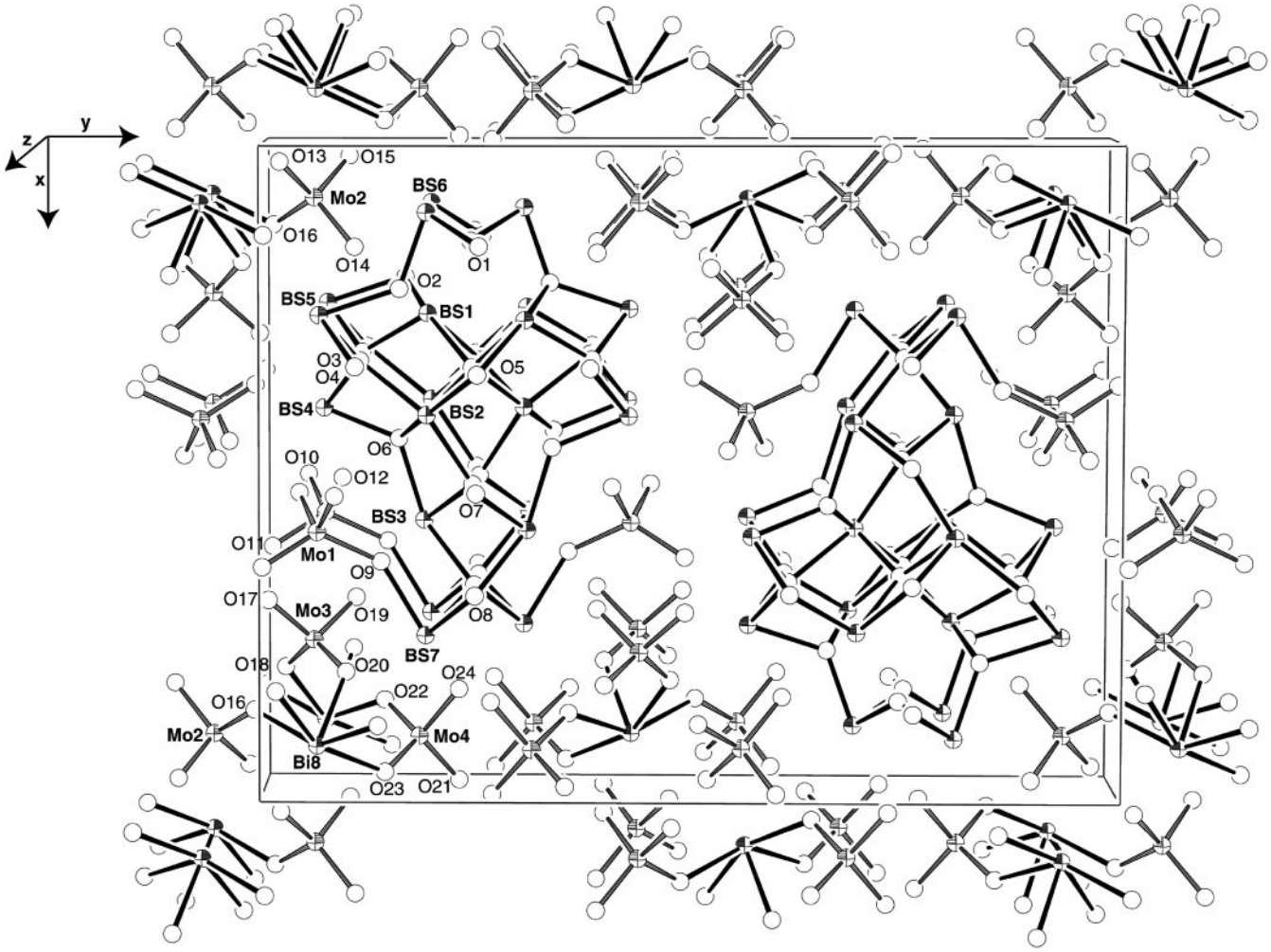

FIG. 1. Perspective view of $Bi_{1.1}Sb_{0.9}MoO_6$ structure.

Both structure refinements resulted in a good agreement between experimental and calculated patterns as can be seen in Fig. 2 and Table 1, with particularly good R values for neutron data (note the $R_{Bragg} = 3.89\%$). Since refined atom positional parameters are rather similar in both cases, the discussion on the structure of $Bi_{1.1}Sb_{0.9}MoO_6$, interatomic distances and bond valences will be based on neutron data analysis that is certainly more reliable.

TABLE 1
Unit-Cell Parameters and Reliability Factors of the Rietveld Refinements of $Bi_{1.1}Sb_{0.9}MoO_6$ Structure (Monoclinic System, Space Group $P\,2_1/c$, $Z = 16$)

	X-ray, Cu$K\alpha$	Neutron, 1.910 Å
a (Å)	17.099(1)	17.0988(7)
b (Å)	22.337(1)	22.3342(9)
c (Å)	5.5699(3)	5.5679(2)
β (°)	90.935(3)	90.926(3)
V (Å^3)	2127.0(2)	2126.0(1)
ρ_{cal} (g.cm^{-3})	6.637	6.640
χ^2	2.93	1.44
R_p (%)	10.3	4.22
R_{wp} (%)	14.0	5.41
R_{Bragg} (%)	7.87	3.89
R_F (%)	3.64	2.26

DISCUSSION

The structure of the parent γ(H) Bi_2MoO_6 and substituted oxides, as described elsewhere (1,7), is built up (Fig. 1) by infinite $[(Bi,Sb)_2O_{14}]$ columns running parallel to the [001] direction (Fig. 3), in a way similar to those columns found in the ionic conductor oxides $Bi(Bi_{12}O_{14})Mo_4VO_{20}$ (14), $Pb(Bi_{12}O_{14})Mo_5O_{20}$ (15), and $Bi(Bi_{12-x}Te_xO_{14})Mo_{4-x}V_{1+x}O_{20}$ (16,17). Such columns are constituted by a nucleus of Bi/Sb1, Bi/Sb2, and O5 while Bi/Sb3 to Bi/Sb6, O1 to O4, O6, and O7 are placed at the outside surface of the column. These units are surrounded by O9–Bi/Sb7–O8 entities, which have been considered as

TABLE 2
Fractional Atom Coordinates, Isotropic Displacement Parameters (Å^2), and Site Occupancies in the Structure of $Bi_{1.1}Sb_{0.9}MoO_6$ (All Atoms are Placed in 4*e* Wyckoff Sites)

	X-ray, Cu$K\alpha$					Neutron, 1.910 Å				
Atom	*x*	*y*	*z*	*B*	Occ.	*x*	*y*	*z*	*B*	Occ.
Bi/Sb1	0.2617(6)	0.1905(5)	0.442(2)	0.8	0.90(3)/0.10(3)	0.2646(8)	0.1920(6)	0.438(2)	0.86(9)	0.90(5)/0.10(5)
Bi/Sb2	0.4121(6)	0.1868(5)	0.917(2)	0.8	0.60(3)/0.40(3)	0.4083(9)	0.1942(7)	0.949(3)	0.86(9)	0.60(5)/0.40(5)
Bi/Sb3	0.5685(7)	0.1981(6)	0.514(2)	0.8	0.28(3)/0.72(3)	0.5812(11)	0.1890(7)	0.520(4)	0.86(9)	0.28(5)/0.72(5)
Bi/Sb4	0.4159(6)	0.0694(5)	0.505(2)	0.8	0.66(2)/0.34(2)	0.4083(9)	0.0714(6)	0.506(3)	0.86(9)	0.66(5)/0.34(5)
Bi/Sb5	0.2631(6)	0.0617(7)	0.007(2)	0.8	0.38(3)/0.62(3)	0.2560(11)	0.0703(8)	0.008(3)	0.86(9)	0.38(5)/0.62(5)
Bi/Sb6	0.1046(7)	0.1979(6)	−0.015(2)	0.8	0.24(3)/0.76(3)	0.1000(10)	0.1940(8)	0.002(3)	0.86(9)	0.24(5)/0.76(5)
Bi/Sb7	0.7415(5)	0.1930(5)	0.985(2)	0.8	0.34/0.66	0.7425(8)	0.1936(7)	1.002(3)	0.86(9)	0.34/0.66
Bi8	0.9119(6)	0.0603(4)	−0.010(2)	0.8	1	0.9128(8)	0.0674(6)	−0.005(3)	0.86(9)	1
Mo1	0.5883(12)	0.0778(8)	0.012(3)	1.1	1	0.5851(11)	0.0677(8)	0.021(3)	0.98(13)	1
Mo2	0.0846(12)	0.0638(9)	0.497(4)	1.1	1	0.0850(11)	0.0596(7)	0.498(3)	0.98(13)	1
Mo3	0.7654(11)	0.0764(9)	0.491(3)	1.1	1	0.7684(9)	0.0588(9)	0.499(3)	0.98(13)	1
Mo4	0.9242(10)	0.1815(8)	0.547(4)	1.1	1	0.9172(11)	0.1832(7)	0.518(4)	0.98(13)	1
O1	0.148	0.245	0.739	0.7	1	0.1477(10)	0.2442(9)	0.740(4)	0.66(6)	1
O2	0.214	0.163	0.064	0.7	1	0.2146(9)	0.1634(9)	0.062(3)	0.66(6)	1
O3	0.330	0.115	0.754	0.7	1	0.3307(12)	0.1157(8)	0.752(4)	0.66(6)	1
O4	0.328	0.114	0.256	0.7	1	0.3283(12)	0.1140(8)	0.256(3)	0.66(6)	1
O5	0.340	0.246	0.747	0.7	1	0.3404(11)	0.2459(9)	0.748(4)	0.66(6)	1
O6	0.453	0.160	0.592	0.7	1	0.4533(12)	0.1597(8)	0.591(3)	0.66(6)	1
O7	0.518	0.247	0.795	0.7	1	0.5185(11)	0.2469(8)	0.794(3)	0.66(6)	1
O8	0.675	0.252	0.233	0.7	1	0.6749(13)	0.2515(9)	0.232(4)	0.66(6)	1
O9	0.633	0.141	0.933	0.7	1	0.6328(11)	0.1414(8)	0.933(4)	0.66(6)	1
O10	0.532	0.044	0.743	0.7	1	0.5328(10)	0.0444(8)	0.741(4)	0.66(6)	1
O11	0.636	0.005	0.104	0.7	1	0.6363(11)	0.0050(8)	0.106(3)	0.66(6)	1
O12	0.525	0.089	0.247	0.7	1	0.5240(10)	0.0902(8)	0.247(3)	0.66(6)	1
O13	0.027	0.021	0.725	0.7	1	0.0274(12)	0.0215(8)	0.725(3)	0.66(6)	1
O14	0.159	0.108	0.622	0.7	1	0.1589(11)	0.1080(9)	0.623(3)	0.66(6)	1
O15	0.023	0.099	0.295	0.7	1	0.0234(11)	0.0994(9)	0.293(4)	0.66(6)	1
O16	0.130	0.009	0.283	0.7	1	0.1304(11)	0.0092(8)	0.284(4)	0.66(6)	1
O17	0.703	0.006	0.605	0.7	1	0.7038(10)	0.0061(8)	0.603(4)	0.66(6)	1
O18	0.820	0.022	0.245	0.7	1	0.8203(10)	0.0222(9)	0.246(3)	0.66(6)	1
O19	0.708	0.108	0.339	0.7	1	0.7078(11)	0.1074(8)	0.342(3)	0.66(6)	1
O20	0.809	0.098	0.762	0.7	1	0.8085(11)	0.0989(9)	0.759(3)	0.66(6)	1
O21	0.991	0.229	0.394	0.7	1	0.9910(11)	0.2295(8)	0.395(4)	0.66(6)	1
O22	0.869	0.141	0.298	0.7	1	0.8697(11)	0.1404(8)	0.300(4)	0.66(6)	1
O23	0.963	0.144	0.759	0.7	1	0.9634(11)	0.1443(9)	0.760(3)	0.66(6)	1
O24	0.840	0.230	0.632	0.7	1	0.8398(10)	0.2303(9)	0.630(4)	0.66(6)	1

ribbons. Finally, there exist isolated Bi8 atoms linked to isolated MoO_4 tetrahedra around the columns.

One of the most interesting features in these materials, and one that could be correlated to their properties, is the location of cations substituting for Bi^{3+} such as Sb^{3+}. This problem has been partially solved by the structural study of representative single crystals of the solid solution $Bi_{2-x}Sb_xMoO_6$ and $Bi_{2-y}As_yMoO_6$ ($x,y = 0.4$) (1). In fact, the stereochemical distribution of the eight bismuth sites is quite different, giving rise to the preferential introduction of antimony or arsenic cations at the outside surface Bi3 to Bi6 of the column and the ribbon Bi7 sites, with very little or no occupancy of the inside column Bi1 and Bi2 and the isolated Bi8 positions (1).

A similar behavior is observed for $Bi_{1.1}Sb_{0.9}MoO_6$, with a higher content of antimony (Table 2). More than 50% occupancy is found in the site at the ribbon (Bi/Sb7) and the outside surface of the column, except for Bi/Sb4 where 34% of the antimony is placed. In contrast, antimony atoms are also placed at the nucleus of the column with 40% in the Bi/Sb2 site, and a small quantity in the Bi/Sb1 position (10%). Comparing these results with the occupancy values of $Bi_{1.6}Sb_{0.4}MoO_6$ and $Bi_{1.6}As_{0.4}MoO_6$ (see Table 3 of Ref. (1)) it is possible to establish a substitution scheme of isovalent ns^2 cations for Bi^{3+}. In the first step, the cations Sb^{3+} and As^{3+} go to the bismuth positions at the ribbon and outside surface of the $[Bi_2O_{14}]$ columns, with no substitution at the sites inside the columns for $Bi_{1.6}As_{0.4}MoO_6$

TABLE 3

Selected Bi/Sb–O, Bi–O, and Mo–O Distances (Å) in the Structure of $Bi_{1.1}Sb_{0.9}MoO_6$ from Neutron Data Rietveld Analysis (e.s.d. = 0.02 Å)

Bi/Sb1–O5	2.17	Bi/Sb2–O5	1.92	Bi/Sb3–O7	2.18
O4	2.29	O6	2.31	O7	2.28
O2	2.32	O7	2.40	O6	2.32
O5	2.46	O5	2.41	O8	2.38
O1	2.66	O3	2.47	O9	2.67
O3	2.70	O4	2.83	O8	2.68
O14	2.82	O7	2.96	O12	2.86
O1	2.89				
Bi/Sb4–O4	2.16	Bi/Sb5–O4	2.08	Bi/Sb6–O1	2.04
O3	2.17	O3	2.16	O1	2.06
O6	2.17	O2	2.22	O2	2.10
O12	2.50	O11	2.57	O21	2.58
O10	2.55	O18	2.80	O23	2.90
O17	2.65	O14	2.82	O15	2.98
O11	2.87	O17	2.83	O21	2.98
		O16	2.99		
Bi/Sb7–O8	2.16				
O9	2.23				
O8	2.25				
O24	2.50				
O19	2.74				
O20	2.78				
O24	2.81				
O22	2.95				
Bi8–O20	2.28				
O23	2.34				
O18	2.36				
O16	2.41				
O22	2.48				
O15	2.60				
O13	2.69				
O13	2.71				
Mo1–O12	1.70	Mo2–O15	1.77		
O11	1.72	O14	1.79		
O10	1.86	O13	1.83		
O9	1.89	O16	1.84		
Mo3–O17	1.72	Mo4–O22	1.75		
O19	1.74	O23	1.77		
O20	1.82	O21	1.78		
O18	1.89	O24	1.81		

or with only a little antimony going to the Bi2 site in $Bi_{1.6}Sb_{0.4}MoO_6$. When the amount of doping element (Sb) increases, as occurs in the $Bi_{1.1}Sb_{0.9}MoO_6$ studied in this work, the antimony content increases in the previously occupied sites and the remaining antimony goes to the unoccupied Bi1 site at the nucleus of the column. It is worth mentioning that bismuth is the only atom found in the isolated Bi8 position in all cases.

All these facts can be explained on the basis of the existence of different coordination polyhedra of bismuth in γ(H) Bi_2MoO_6. In this last case, Bi8 atoms are coordinated to five oxygens at rather regular distances between 2.3 and 2.4 Å and then to three other oxygen atoms at longer distances $\approx$2.7 Å. Bi1 to Bi7 show a very irregular coordination with three or four oxygen atoms at distances ranging between 2.1 and 2.5 Å and three or four other oxygens at longer distances ($>$ 2.6 Å), the average of the Bi1–O short distances being longer than any of the Bi–O short distance averages for the other Bi atoms. For this reason, the Bi8 position is never occupied by smaller cations like Sb^{3+} or As^{3+} ($r_{Bi^{3+}} = 1.03$ Å, $r_{Sb^{3+}} = 0.76$ Å, and $r_{As^{3+}} = 0.58$ Å (18)) and Bi1 is only slightly substituted for, and only at high substitution degree, as is observed in the $Bi_{1.1}Sb_{0.9}MoO_6$ reported in this work. Moreover, the Bi1 and Bi2 positions inside the columns are so to speak "protected" against substitution by cations possessing a more stereoactive lone pair of electrons than $6s^2$ of Bi^{3+} (Sb^{3+}, $5s^2$; As^{3+}, $4s^2$) (19). So in $Bi_{1.1}Sb_{0.9}MoO_6$ bismuth/antimony–oxygen short distance ($<$ 2.5 Å) change, giving rise also to very irregular coordination for Bi/Sb1 to Bi/Sb7, which became bonded to three (Bi/Sb4, Bi/Sb5, Bi/Sb6, and Bi/Sb7) or four (Bi/Sb1 and Bi/Sb3) or even to five oxygens (Bi/Sb2). In contrast, the Bi8 atom, which is not substituted for Sb, remains coordinated to the same five oxygens. If $x > 0.9$ values are tried for the solid solution $Bi_{2-x}Sb_xMoO_6$, a mixture of phases, including Sb_2MoO_6, is obtained (1). The Sb_2MoO_6 structure (20) resembles not γ(H) Bi_2MoO_6 but the

TABLE 4

Bond-Valence Values for Bi, Bi/Sb–O, and Mo Atoms of γ(H)-Bi_2MoO_6, $Bi_{1.6}Sb_{0.4}MoO_6$, $Bi_{1.6}As_{0.4}MoO_6$ (1), and $Bi_{1.1}Sb_{0.9}MoO_6$ Oxides

	Site			
	γ(H)-Bi_2MoO_6	$Bi_{1.6}Sb_{0.4}MoO_6$	$Bi_{1.6}As_{0.4}MoO_6$	$Bi_{1.1}Sb_{0.9}MoO_6$
Bi1	2.86	2.79	2.69	
Bi/Sb1				2.86
Bi2	2.85	2.91	2.87	
Bi/Sb2				3.16
Bi3	3.02			
Bi/Sb3		2.80		2.30
Bi/As3			2.71	
Bi4	3.20			
Bi/Sb4		3.10		3.06
Bi/As4			2.79	
Bi5	3.13			
Bi/Sb5		2.84		2.73
Bi/As5			2.71	
Bi6	3.25			
Bi/Sb6		2.94		2.92
Bi/As6			2.44	
Bi7	2.99			
Bi/Sb7		2.84		2.48
Bi/As7			2.67	
Bi8	2.96	2.98	2.92	3.00
Mo1	5.5	5.5	5.4	5.2
Mo2	5.3	5.3	5.4	4.8
Mo3	5.2	5.2	5.1	5.1
Mo4	5.3	5.4	5.3	5.2

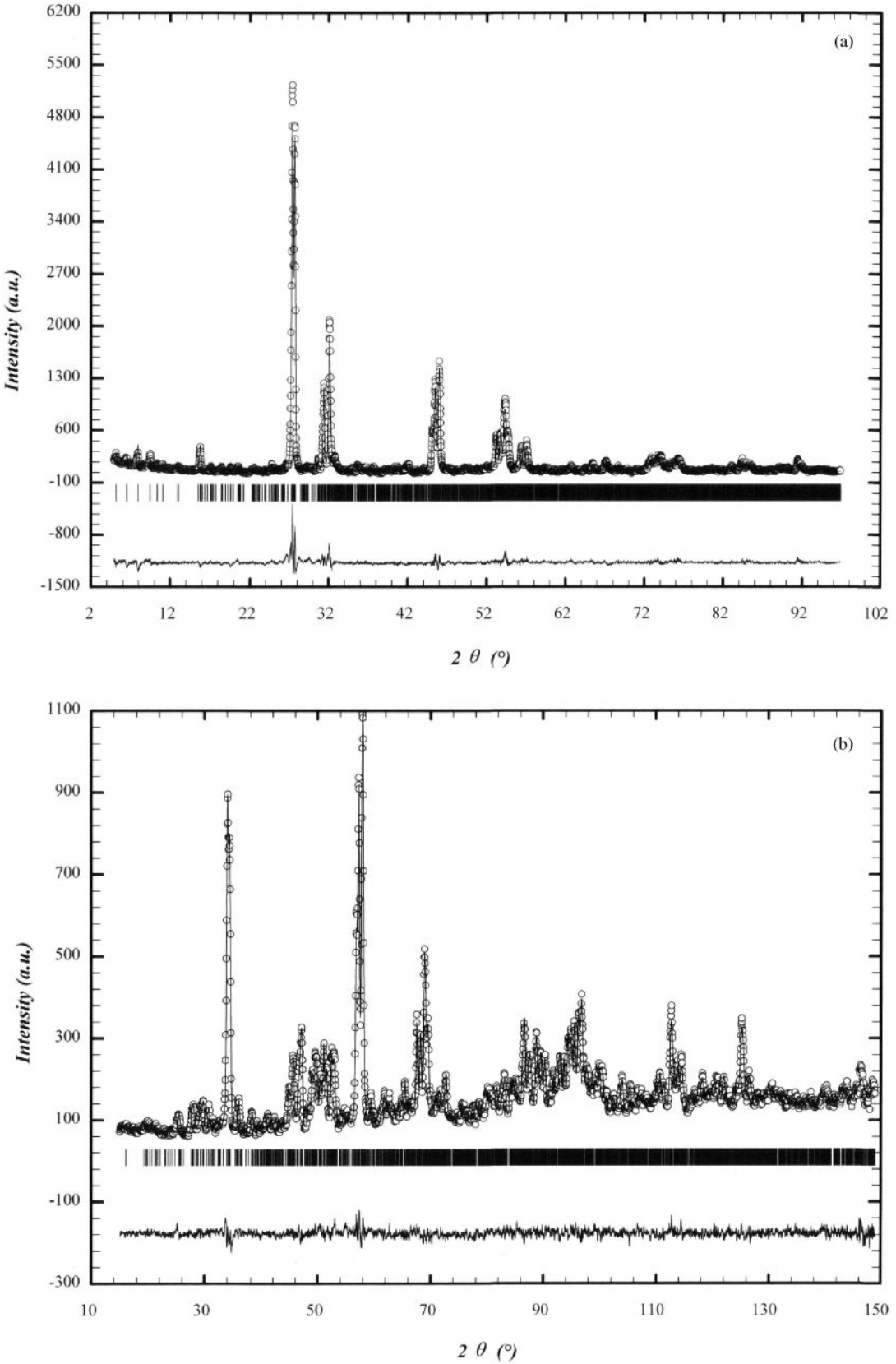

FIG. 2. Observed (○), calculated (solid line), and difference (lower full line) diffraction patterns for $Bi_{1.1}Sb_{0.9}MoO_6$: (a) X-ray and (b) neutron refinements. Vertical bars at the bottom indicate the Bragg positions.

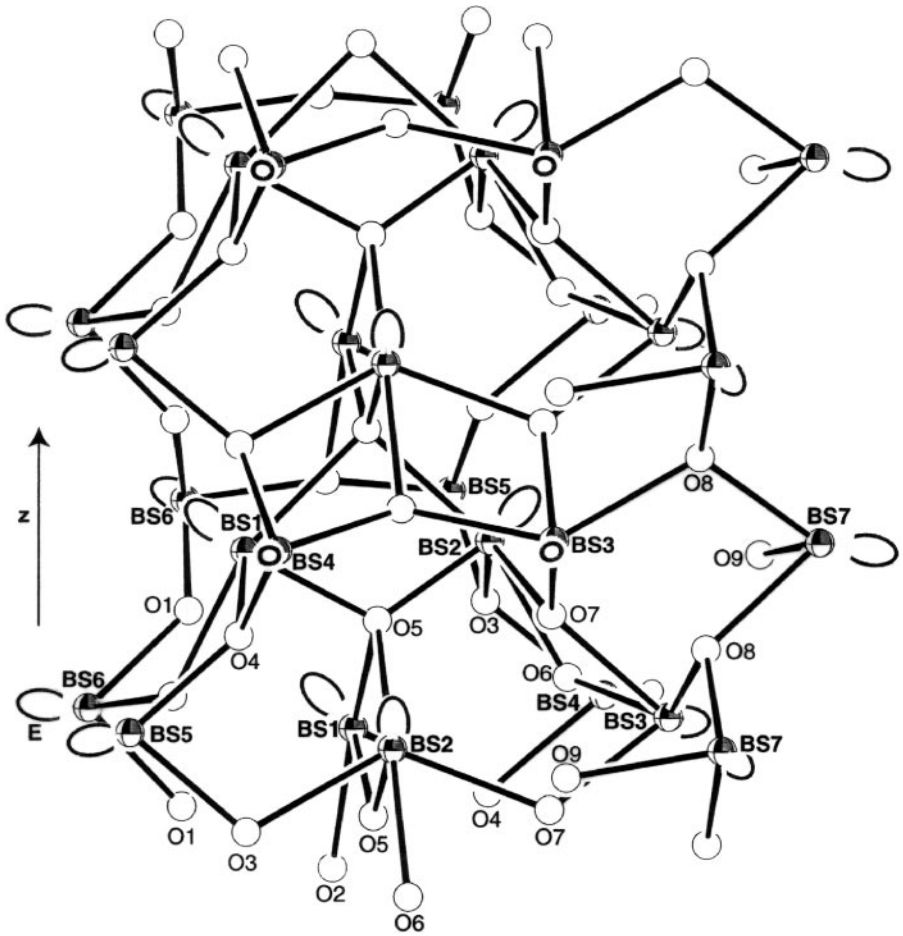

FIG. 3. Bi1 to Bi7 coordinations in the [001] direction of the $Bi_{1.1}Sb_{0.9}MoO_6$ structure (E, $6s^2$ Bi^{3+} lone pair of electrons).

low-temperature form γ(L) Bi_2MoO_6, being closely related to the $n = 1$ Aurivillius structural type, where Sb atoms exhibit an open coordination.

The molybdenum coordination is less affected by antimony substitution in $Bi_{1.1}Sb_{0.9}MoO_6$, with Mo–O bond distances ranging from 1.70 to 1.89 Å and mean values of 1.79 Å for Mo1 and Mo3, 1.81 Å for Mo2, and 1.78 Å for Mo4.

Using the bond-valence criterion (21) (Table 4) it can be observed that for the parent γ(H) Bi_2MoO_6 oxide the bond valences of bismuth atoms are close to the expected value of 3, while they are smaller for substituted $Bi_{1.6}Sb_{0.4}MoO_6$ and $Bi_{1.6}As_{0.4}MoO_6$, showing underbonding as a general trend. This fact is particularly important in the arsenic phase, which represents the upper limit of the $Bi_{2-y}As_yMoO_6$ solid solution, where some Bi/As bond-valence values are lower than 2.5. In the same way, in $Bi_{1.1}Sb_{0.9}MoO_6$ oxide two Bi/Sb positions become strongly underbonded. Thus, it could be inferred that substitution can advance up to a minimum underbonding value for bismuth/antimony–oxygen and then the structure breaks down.

The bond-valence values for molybdenum atoms (Table 4) show less overbonding than those observed for the previously studied phases, but always remaining close to the expected value of 5.

In conclusion, the structure of $Bi_{1.1}Sb_{0.9}MoO_6$ (space group $P2_1/c$, $a = 17.0988(7)$ Å, $b = 22.3342(9)$ Å, $c = 5.5679(2)$ Å, and $\beta = 90.926(3)^\circ$) has been refined using both X-ray and neutron powder diffraction techniques. This oxide is isostructural with the high-temperature polymorph (γ(H)) of Bi_2MoO_6. It is deduced from the analysis of structural data that antimony replaces bismuth atoms in their positions in an ordered way: (1) first, bismuth atoms located at the outside surface of the columns and the ribbon are replaced, followed by (2) bismuth atoms inside the columns with shorter Bi–O distances, and then by (3) bismuth atoms inside the columns with longer Bi–O distances; (4) the isolated bismuth atoms with more regular coordination and longer mean Bi–O distance are never substituted. These facts can be explained on the basis of the different stereochemical behavior of $6s^2$ and $5s^2$ lone-pair electrons associated with Bi^{3+} and Sb^{3+}, respectively, and the

possible decrease of Bi/Sb–O distances. The Bi:Sb ≡ 1.1:0.9 ratio has been verified by structural refinement and represents the upper limit of the solid solution $Bi_{2-x}Sb_xMoO_6$. From a structural point of view this limit could be understood in the light of the bond-valence method. When high antimony (or arsenic) substitution is achieved, the bond-valence values for bismuth-substituted sites drastically decrease, leading to strong underbonded states, but beyond the established limit higher underbonding cannot be accepted and the structure breaks down.

ACKNOWLEDGMENTS

The authors are grateful to ILL for making all facilities available. They acknowledge fruitful discussions with Prof. J. E. Iglesias (ICMM/CSIC, Spain), Dr. J. Galy (CEMES/CNRS, France), and Dr. M. T. Fernández-Díaz (ILL, France). A.C. and P.B. appreciate the financial support of DGICYT and CAM of Spain under projects MAT97-0711 and 07N/0061/1998, respectively. P.B. thanks the Spanish Government for the grant awarded.

REFERENCES

1. P. Bégué, R. Enjalbert, J. Galy, and A. Castro, *Solid State Sci.* **2,** 637 (2000).
2. H. Kodama and A. Watanabe, *J. Solid State Chem.* **56,** 225 (1985).
3. P. Bégué, P. Millán, and A. Castro, *Bol. Soc. Esp. Ceram. Vidr.* **38,** 558 (1999).
4. A. F. Van den Elzen and G. D. Rieck, *Acta Crystallogr. B* **29,** 2436 (1973).
5. F. Theobald, A. Laarif, and A. W. Hewat, *Ferroelectrics* **56,** 219 (1984).
6. G. Sankar, M. A. Roberts, J. Meurig Thomas, G. U. Kulkarni, N. Rangavital, and C. N. R. Rao, *J. Solid State Chem.* **119,** 210 (1995).
7. D. J. Buttrey, T. Vogt, U. Wilgruber, and W. R. Robinson, *J. Solid State Chem.* **111,** 118 (1994).
8. D. H. Galvan, S. Fuentes, M. Avalos-Borja, L. Cota-Araiza, E. A. Early, M. B. Maple, and J. Cruz-Reyes, *J. Phys. Condensed Matter A* **217,** 5 (1993).
9. D. D. Agarwal, K. L. Madhok, and H. S. Gosami, *React. Kinet. Catal. Lett.* **52,** 225 (1994).
10. G. Chiodelli, A. Magistris, G. Spinolo, C. Tomasi, V. Antonucci, and N. Giordano, *Solid State Ionics* **74,** 37 (1994).
11. I. H. Ismailzade, I. M. Aliyev, R. M. Ismailzov, A. I. Alekberov, and D. A. Rzayev, *Ferroelectrics* **22,** 853 (1979).
12. M. F. Portela, C. Pinheiro, C. Dias, and M. J. Pires, *Stud. Surf. Sci. Catal.* **67,** 77 (1991).
13. J. Rodríguez-Carbajal, Fullprof, Version 0.2, Mars 98, Laboratoire Leon Brillouin (CEA-CNRS), Saclay, France, 1998.
14. R. Enjalbert, G. Hasselmann, and J. Galy, *J. Solid State Chem.* **131,** 236 (1997).
15. R. Enjalbert, G. Hasselmann, and J. Galy, *Acta Crystallogr. C* **53,** 269 (1997).
16. A. Castro, R. Enjalbert, P. Baules, and J. Galy, *J. Solid State Chem.* **139,** 185 (1998).
17. P. Bégué, J. M. Rojo, R. Enjalbert, J. Galy, and A. Castro, *Solid State Ionics* **112,** 275 (1998).
18. R. D. Shannon, *Acta Crystallogr. A* **32,** 751 (1976).
19. J. Galy, G. Meunier, S. Andersson, and A. Åström, *J. Solid State Chem.* **13,** 142 (1975).
20. A. Castro, R. Enjalbert, and J. Galy, *Acta Crystallogr. C* **53,** 1526 (1997).
21. D. Altermatt and D. Brown, *Acta Crystallogr. B* **41,** 240 (1985).